INTERNATIONAL JOURNAL FOR NUMERICAL AND ANALYTICAL METHODS IN GEOMECHANICS
Int. J. Numer. Anal. Meth. Geomech., **23**, 829–843 (1999)

LAYERED ELASTIC MODEL FOR ANALYSIS OF CONE PENETRATION TESTING

ZHONG QI YUE[1] AND JIAN-HUA YIN[2,*]

[1]*Halcrow Asia Partnership Ltd., 23rd Floor, Central Plaza, 18 Harbour Road, Hong Kong, China*
[2]*Department of Civil & Structural Engineering, Hong Kong Polytechnic University, Hung Hom, Kowloon, Hong Kong, China*

SUMMARY

A layered elastic model is adopted in the paper for the analysis of soil layering effects on the results of Cone Penetration Testing (CPT). Analytical solutions associated with the layered elastic CPT model and obtained via numerically integrating the fundamental singular solution for layered elastic solids due to the action of a body force concentrated on a circular ring. The soil layering effects on the CPT tip and friction resistance are examined in detail using the layered elastic CPT model. These examinations include parametric studies, influence of soil compressibility, comparisons with theoretical results given in the literature, verification with experimental data and simulation of field trial results. The examinations lead to the conclusions that the layered elastic CPT model can be used to analyse soil layering effects on CPT results and to estimate relative shear modulus strength of soil layers. Copyright © 1999 John Wiley & Sons, Ltd.

Key words: cone penetration test; layered elastic model; elasticity; shear modulus; cone tip resistance; sleeve friction resistance

INTRODUCTION

A layered elastic model is usually used to represent layered ground soils as a system of horizontally placed and linearly elastic layers, and to describe the elastic component of soil deformation. The non-linearity and stress-dependent load response of soils cannot be directly represented by a layered elastic model. Within the limitation of the assumptions, the layered elastic model is generally considered to be the most practical theoretical approach to the analysis of layered soil under loads. For example, the layered elastic models have been extensively used in the design and analysis of pile foundations and pavement structures.[1–6]

Classical studies related to layered elastic models are given by Burmister[7,8] for the applications to two- and three-layered pavement structures subject to traffic loads. Since the classical studies, the models have been extended by various researchers to cover multi-layered elastic systems subject to various types of external and internal loads.[9–12] In particular, a concise and rigorous statement has been recently given by Yue[10] for the fundamental singular solution of concentrated body-force actions in layered elastic solids.

* Correspondence to: J.-H. Yin, Department of Civil & Structural Engineering, Hong Kong Polytechnic University, Hung Hom, Kowloon, Hong Kong, China

Contact grant sponsor: Hong Kong Polytechnic University

CCC 0363–9061/99/080829–15$17.00

Received 16 February 1998
Revised 23 September 1998

The purpose of this note is to apply a layered elastic model to the analysis of static Cone Penetration Testing (CPT) results. The CPT is one of the widely used *in situ* testing methods in geotechnical engineering and is the most popular routine ground investigation technique that provides an accurate continuous profile of soil stratification.[13–15] In the CPT, a cone on the end of a series of rods is pushed into the ground at a constant rate. Continuous measurements can be obtained for the components of penetration resistance including cone tip resistance, sleeve friction resistance and friction ratio. Such penetration resistance is developed during the steady slow penetration of the cone into soils. The CPT measurements can be applied to delineation of the soil profile and to the evaluation of the soil engineering parameters. The CPT measurements, however, may be significantly affected by soil layering. Observations and experience indicate that the CPT resistance responds to soil layering within 5–10 cone diameters above and below the cone. Such layering effect can lead to some imprecision in locating soil interfaces and in evaluating soil parameters.[13,14]

It is well known that during cone penetration testing, large plastic deformation must occur near the cone tip. Consequently, a layered elastic model may appear to be an extremely poor model for the interpretation of CPT results. This applicability concern has been well discussed in a seminal study recently carried out by Vreugdenhil *et al.*[16] In the study, Vreugdenhil *et al.*[16] demonstrated that the cone tip resistance senses the presence of a nearby layer elastically and that an elastic analysis is suitable to examine the layering effect on cone tip resistance. Similar to the study of Vreugdenhil *et al.*[16] the present study also concentrates on the analysis of soil layering effect on the CPT results. The actual process of large plastic deformation in the surrounding soils closely adjacent to the cone tip may be examined by using non-linear and large strain finite element methods.[17,18]

The elastic analysis of soil layering effect on cone tip resistance, carried out by Vreugdenhil *et al.*[16] was based on a simple and approximate solution in an incompressible layered elastic soil. The cone tip was modeled as a body-force load uniformly distributed over a disc-shaped area of the cone radius. The flexibility relationship between the body-force, load and the vertical displacement at the centre of the disc-shaped area was used to analyse the cone tip resistance. For simplicity, the relationship was formulated approximately using the Boussinesq point-load solution in a homogeneous half-space together with an approximation suggested by Poulos[20] for combining the relative displacements in two elastic layers. The assumption of soil incompressibility was also employed in the formulation. As a result, the elastic analysis was mainly focused on the undrained deformation of saturated cohesive soils induced by cone tip penetration.

The present study is intended to extend and refine the CPT elastic analysis carried out by Vreugdenhil *et al.*[16] In order to achieve the objective, this study presents an exact layered elastic solution for the analysis of cone tip resistance in both compressible and incompressible layered soils. Furthermore, this study also presents a layered elastic model and an associated solution for the analysis of cone sleeve friction resistance in layered soils. As a result, the layering effects on both the cone tip resistance and sleeve friction resistance can be examined in the framework of linear elasticity. The compressible deformation of cohesionless and cohesive soils during cone penetration can be taken into account in the elastic analysis of the layering effects. Results of the analyses presented in the study indicate that the layered elastic models can be applied to the interpretation of cone tip resistance and sleeve friction resistance in layered soils.

LAYERED ELASTIC MODEL

Model for CPT analysis

Figure 1 illustrates a friction-cone penetrometer steady penetrating into a layered ground soil. Surface of the layered elastic soil is free of loading. The layered soil is modelled as a system of horizontally placed and linearly elastic layers. The interface between any two connected layers is assumed to be completely bonded. Each elastic layer has two elastic constants which can be expressed in terms of shear modulus (μ) and Poisson's ratio (v). The soil compressibility can be modeled using the value of Poisson's ratio between 0 and 0·5. If Poisson's ratio is equal to 0·5, the elastic soil layer is incompressible and represents undrained deformation of fully saturated cohesive soils. If Poisson's ratio is not equal to 0·5, the elastic soil layer is compressible and represents drained deformation of other type of soils such as sand.

The radius of the cone is a and the length of the cone sleeve is l. The cone tip resistance and the sleeve friction are represented by two body-forces acting in vertical direction. The cone tip resistance is represeted by a body-force pressure uniformly distributed over a disc-shaped area of the cone radius a, as used by Vreugdenhil *et al.*[16] On the other hand, the cone sleeve friction resistance is represented by a body-force q uniformly distributed over a hallow cylinder surface of the cone radius a and the cone friction sleeve height l. Consequently, the following expressions can be used to represent the loading of the cone tip resistance and the sleeve friction in a layered elastic solid in the cylindrical co-ordinate system ($r\theta z$) (Figure 1).

For tip resistance, we have

$$f_t(r, z) = p\delta(z - h)H(a - r) \tag{1}$$

For sleeve friction resistance, we have

$$f_s(r, z) = q\delta(r - a)[H(z - h + l) - H(z - h)] \tag{2}$$

where p is the body force intensity representing cone tip resistance q_c, q the body force intensity representing cone sleeve friction resistance, f_s, $\delta(\ )$ a Dirac delta function, $H(\ )$ a Heaviside step function, h the depth of a cone tip in the layered elastic solid.

Solution for CPT analysis

The above model for the CPT analysis forms boundary-value problems in a layered elastic solid subject to the two body- forces. The solutions for the boundary-value problems in the framework of linear elasticity can be constructed by integrating the fundamental solutions associated with body forces concentrated at a point or uniformly concentrated along a circular ring over the loaded surfaces. The circular ring is parallel to the interface planes of the layered elastic solids.

As discussed previously, Yue[10] presented a rigorously mathematical and analytical study of solutions for the static responses of a layered elastic solid subjects to the point and ring types of concentrated body-forces. In this study, the fundamental solution for the layered elastic solid subject to the ring-type of concentrated body-forces is used to formulate the exact solutions for the CPT analyses.

For a layered elastic solid subject to the body-force $f_t(r, z)$ in (1), the solution of the displacement $[u_r, u_\theta, u_z]^T$, the vertical stress $[\sigma_{rz}, \sigma_{\theta z}, \sigma_{zz}]^T$ and the plane strains $[\varepsilon_{rr}, \varepsilon_{r\theta}, \varepsilon_{\theta\theta}]^T$ can be

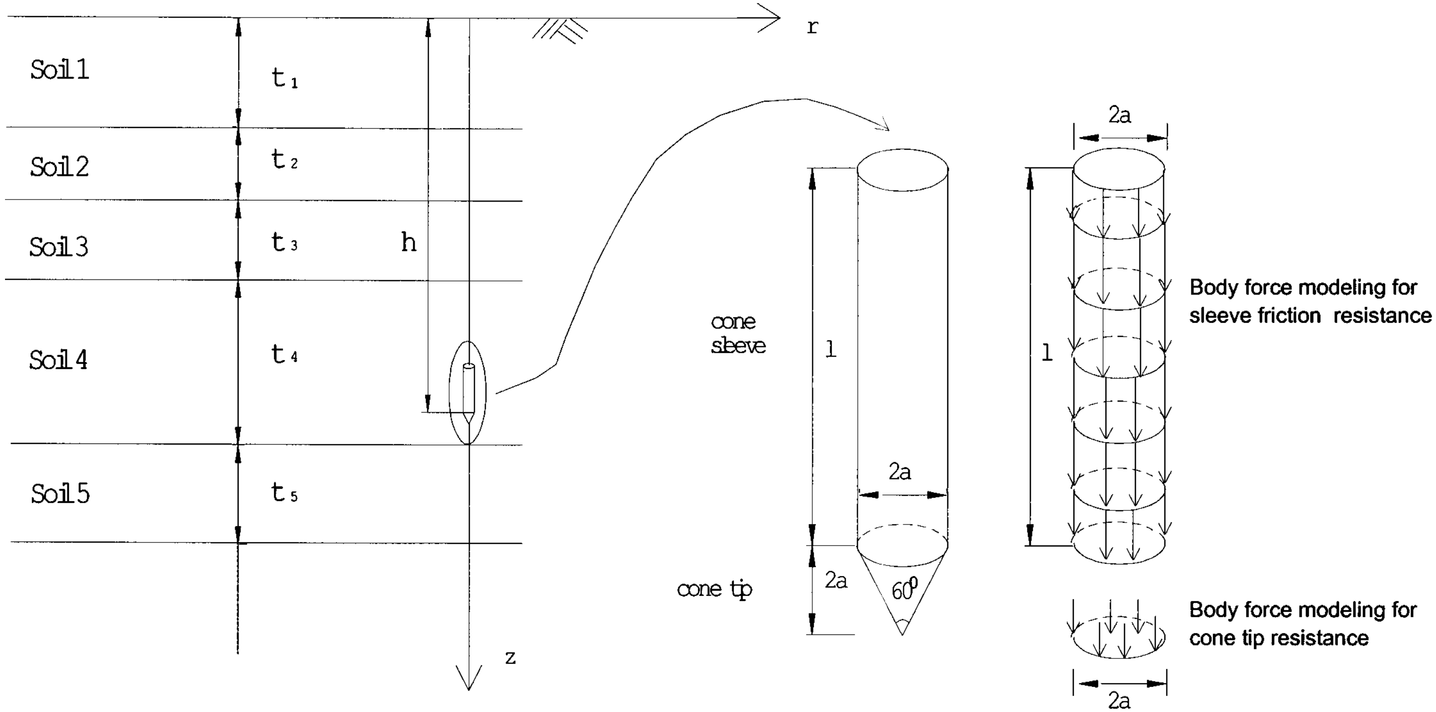

Figure 1. A layered elastic model for a friction cone penetrating into layered soils

obtained by integrating the fundamental solution $\mathbf{G}_s$ over the loaded circular area and expressed as follows:

$$\mathbf{U}_{ts}(r, z, h) = 2\pi p \int_0^a \mathbf{G}_s(r, r_0, z, h)\mathbf{I} r_0 \, dr_0 \tag{3}$$

where (i) for $\mathbf{U}_{ts} = [u_r, u_\theta, u_z]^T$, $\mathbf{G}_s = \mathbf{G}_u$; (ii') for $\mathbf{U}_{ts} = [\sigma_{rz}, \sigma_{\theta z}, \sigma_{zz}]^T$, $\mathbf{G}_s = \mathbf{G}_z$; (iii) for $\mathbf{U}_{ts} = [\varepsilon_{rr}, \varepsilon_{r\theta}, \varepsilon_{\theta\theta}]^T$, $\mathbf{G}_s = \mathbf{G}_p$; and $\mathbf{I} = [0, 0, 1]^T$. The superscript T stands for the transpose of a matrix.

Similarly, the layered elastic solution for the body-force representing the cone sleeve friction resistance in (2) can be obtained by integrating the fundamental solution $\mathbf{G}_s$ over the loaded circular cylinder surface and expressed as follows:

$$\mathbf{U}_{fs}(r, z, h) = 2\pi a q \int_0^l \mathbf{G}_s(r, a, z, h - t)\mathbf{I} \, dt. \tag{4}$$

where (i) for $\mathbf{U}_{fs} = [u_r, u_\theta, u_z]^T$, $\mathbf{G}_s = \mathbf{G}_u$; (ii) $\mathbf{U}_{fs} = [\sigma_{rz}, \sigma_{\sigma z}, \sigma_{zz}]^T$, $\mathbf{G}_s = \mathbf{G}_z$; and (iii) for $\mathbf{U}_{fs} = [\varepsilon_{rr}, \varepsilon_{r\theta}, \varepsilon^{\theta\theta\sigma}]^T$, $\mathbf{G}_s = \mathbf{G}_p$.

In equations (3) and (4), the $\mathbf{G}_u$, $\mathbf{G}_z$, and $\mathbf{G}_p$ are the fundamental solutions associated with the ring loading which have been well discussed and evaluated by Yue.[10] Numerical evaluation indicated that there is no problem in the calculations of the fundamental solution with very high accuracy and efficiency. In particular, the singular terms of the fundamental solution were given in exact closed forms. The solution of the plane stresses $[\sigma_{rr}, \sigma_{\theta r}, \sigma_{\theta\theta}]^T$ and the vertical strains $[\varepsilon_{rz}, \varepsilon_{\theta z}, \varepsilon_{zz}]^T$ can be easily obtained by using the constitutive equation of linear elasticity.

Numerical evaluation

Computer programs have been written to calculate the solutions for CPT analysis in equations (3) and (4) on a personal computer environment. The definite integrals in equations (3) and (4) are evaluated using an adaptively iterative Simpson's quadrature. Since the fundamental solutions can be accurately and efficiently calculated, the calculation of the solutions for CPT analysis in equations (19) and (20) is a straightforward task for any evaluation points except the source points located exactly on the loaded circular area or the loaded cylinder surface. At these source points, the fundamental solutions for the displacements and for the stresses may have the weak singularity of $\ln R$ and the singularity of $1/R$, respectively,[10,20] The closed-form singular terms of the fundamental solution can be used to overcome the above singularity issue in the numerical integration by analytically integrating the definite integrates in (3) and (4) associated with the singular terms.

Examples are given in the following to illustrate the variations of the vertical displacement u_z induced by the CPT body-forces p or q since u_z shall be of use in the CPT analysis. A bi-material elastic solid of infinite extent is used in the examples. The cone tip is located at the bi-material interface. The ratio of the cone sleeve length l over the cone tip radius a is equal to 7·492 (= 133·74 mm/17·85 mm).[15] Figure 2 illustrates the distribution of u_z in the bi-material solid induced by the cone tip body force p. Figure 3 illustrates the distribution of u_z in the bi-material solid induced by the cone sleeve friction body force q. From these two figures, it can be observed that the maximum u_z induced by p is located at the centre of the loaded circular area and that the u_z induced by q is mainly dependent on the z for any points within the loaded cylinder surface.

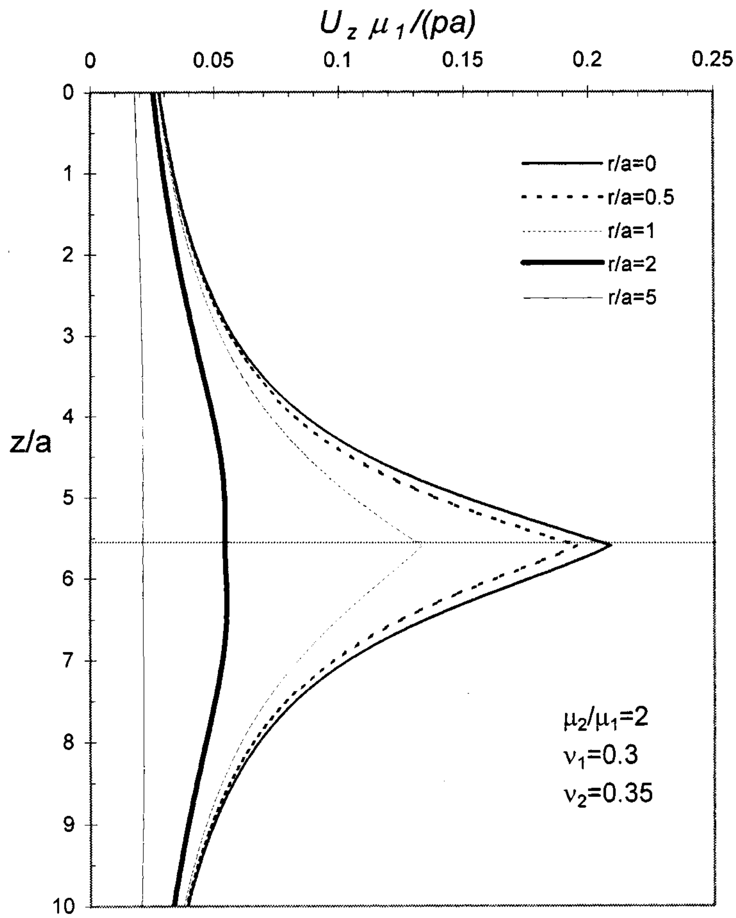

Figure 2. Distribution of the vertical displacement u_z induced by CPT tip resistance p at a bi-material soil interface with the vertical co-ordinate z/a

ANALYSIS OF TIP RESISTANCE

General

Cone tip resistance q_c is the resistance to penetration developed by the cone and is equal to the vertical force applied to the cone divided by its horizontally projected area. As suggested by Vreugdenhil *et al.*[16] we adopt the following non-dimensional penetration resistance to analyse the layering effect on the cone tip resistance,

$$\eta = \frac{pa}{\mu_1 U_p} \tag{5}$$

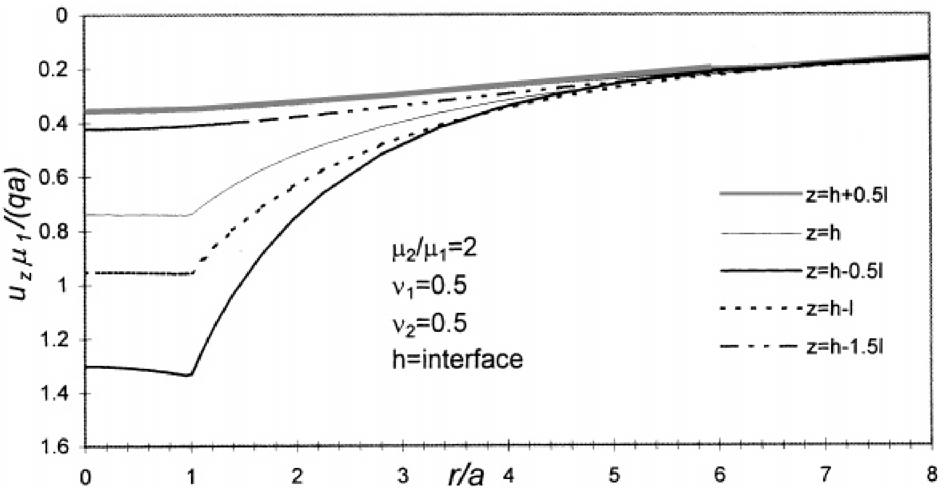

Figure 3. Distribution of the vertical displacement u_z induced by CPT friction resistance q at a bi-material soil interface with the radial distance z/a

where U_p is the maximum value of the vertical displacement u_z induced by the cone tip body force p. U_p is evaluated at the centre of the loaded circular area (i.e. $r = 0$, $z = h$) as illustrated in Figure 2.

The non-dimensional penetration resistance η is a function of the location of cone tip position h/a and the material parameters of the layered elastic soils. These material parameters include the shear modulus ratio μ_i/μ_1, Poisson's ratio ν_i, and the non-dimensional layer thickness t_i/a, where the subscript i stands for the ith layer in a multilayered elastic soil system. The non-dimensional penetration resistance η, as a function of the cone tip location in a layered elastic soil, will be used to simulate the variations of the cone tip resistance q_c measured in a layered soil.

Results and analysis

As discussed previously, an elastic analysis has been carried out by Vreugdenhil *et al.*[16] for the layering effect on cone tip resistance in incompressible soils under undrained condition such as fully saturated cohesive soils. A simple and approximate solution was used in the analysis. Examples are given below to compare the results given by Vreugdenhil *et al.*[16] to those obtained using the present layered elastic solution.

Figure 4 illustrates the variations of the non-dimensional cone penetration resistance η as a cone moves downward through material 1, crosses the interface, and continues into material 2. The bi-material interface is located at a non-dimensional depth zero. The non-dimensional depth h/a in Figure 4 is measured positive upward. It can be observed that the approximate solution given by Vreugdenhil *et al.*[16] gives results (i.e. Figure 5 in Vreugdenhil *et al.*[16]) close to those given by the present layered elastic solution, although the discrepancy between the two solutions is greater when the cone enters into the stiffer material 2. It can also be observed that the maximum gradient of the variation in η value occurs once the cone tip locates at the bi-material

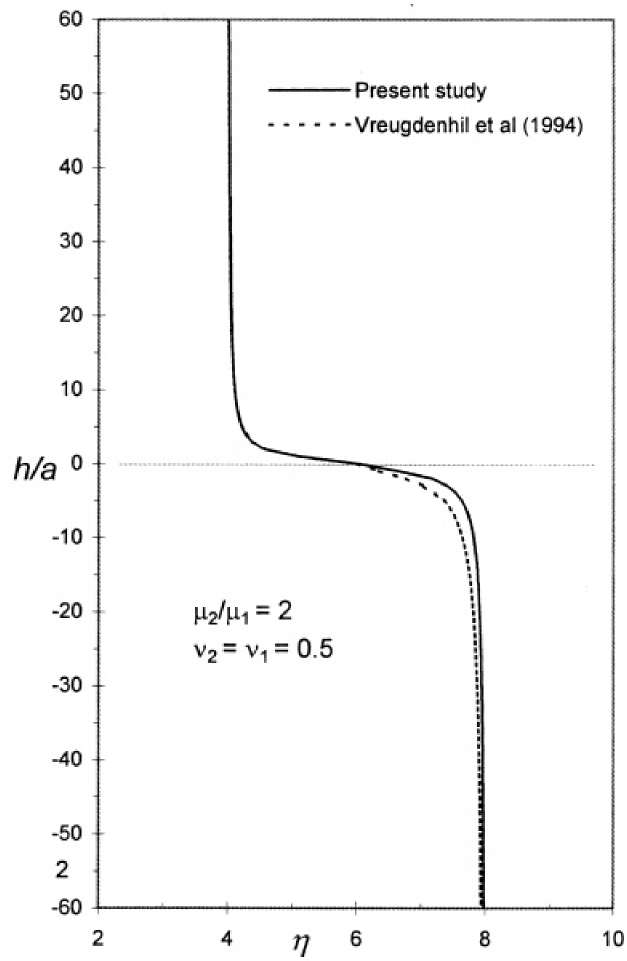

Figure 4. Variations of the non-dimensional cone penetration resistance η with the cone depth in a bi-material soil

interface. The present results are almost exactly the same as those in Figure 5 given by Vreugdenhil *et al.*[16] using an exact solution.

In the study given by Vreugdenhil *et al.*,[16] results obtained using the approximate solution were also compared with those measured in a calibration chamber.[21,2] Figure 5 shows one of the comparison examples. In this example, a soft layer was sandwiched between two stiffer layers. The stiffness ratios used by Vreugdenhil *et al.*[16] to model the experimental results were $\mu_2/\mu_1 = 0{\cdot}34$ and $\mu_3/\mu_2 = 2{\cdot}51$. Results obtained using the present solution for the three layered elastic soils with a free surface at $h/a = 0$ and a rigid base $h/a = 70$ are also plotted in Figure 5. It can be observed from Figure 5 that comparing to the results given by Vreugdenhil *et al.*,[16] the present results are closer to the experimental data.

The above elastic analysis of the layering effect on the cone tip resistance is limited due to the assumption that the layered soils are incompressible. Further analyses are given below to illustrate the effect of soil compressibility of the cone tip resistance. Compressible soil deformation

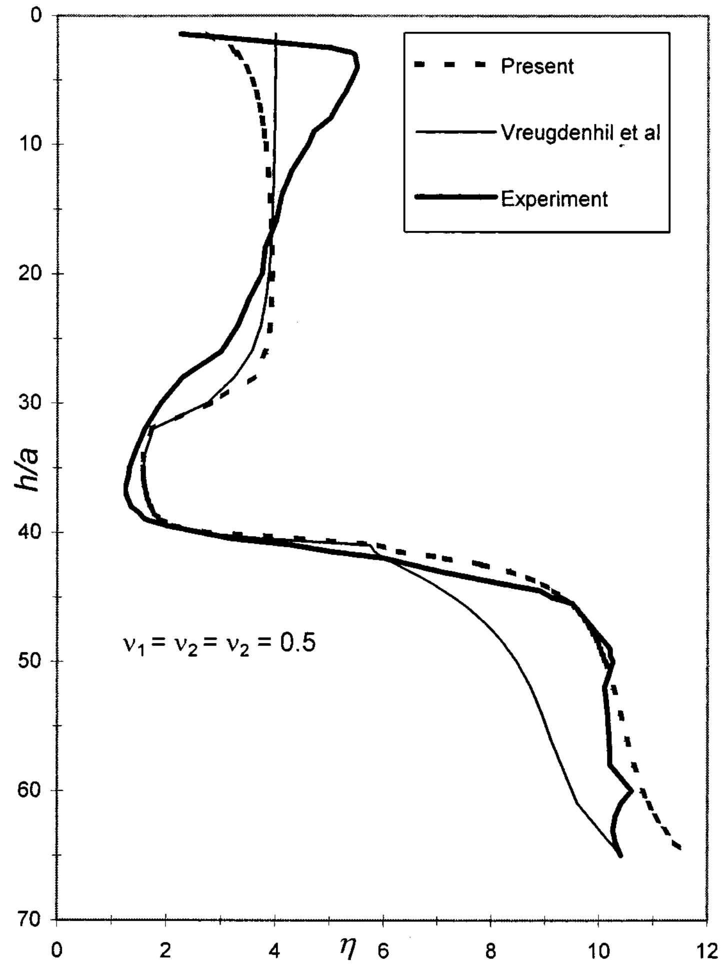

Figure 5. Comparison of the present results with others' theoretical and experimental results for cone tip resistance in a three layer soil

can occur in the situation where the soil is partially saturated or has a drained condition. Elastic analysis of compressible soil deformation can be realized by using a value of Poisson's ratio v less than 0·5. Numerical results indicate that for v is equal to 0·0, 0·1, 0·2, 0·3, 0·4, or 0·5, the η is equal to 2·76, 2·86, 2·99, 3·188, 3·48 or 4·0, respectively. It can be observed that the η is increasing up to 32 per cent with the increase of Poisson's ratio from 0 to 0·5 in a homogeneous soil.

ANALYSIS OF SLEEVE FRICTION

General

Cone sleeve friction resistance f_s is the soil resistance to penetration developed by the friction sleeve and is equal to the vertical force applied to the sleeve divided by its surface area. This

resistance consists of the sum of friction and adhesion mobilized on the sleeve cylindrical surface. Similar to the analysis of cone tip resistance, we adopt the following non-dimensional sleeve friction to analyse the layering effect on the cone sleeve friction resistance:

$$\zeta = \frac{qa}{\mu_1 U_q} \tag{6}$$

where U_q is a representative value of the vertical displacement u_z induced by the sleeve friction body force q. As illustrated in Figure 3, the u_z varies with the z-axis and keeps almost constant with the r-axis within the loaded hollow cylindrical region. Numerical analysis indicates that the U_q at the cone center point ($r = 0$, $z = h = 0{\cdot}5l$) can be adopted as the representative value.

Similar to the η, the ζ is a function of the location of cone tip position h/a and the material parameters of layered elastic soils. The ζ, as a function of the cone tip location in a layered elastic soil, will be used to simulate the variations of sleeve friction resistance f_s measured in layered soils.

Results and analysis

Figure 6 shows the variations of the ζ with the h/a as a cone penetrates downward through material 1, crosses the interface, the continues into material 2. Following three observations can be made from the figure:(a) the maximum increase in ζ value is proportional to the shear modulus ratio μ_2/μ_1; (b) the transient zone around the interface is about 10–15 times of the cone radius a; and (c) the maximum gradient of the variation in ζ value is located at about $0{\cdot}5l$, i.e. half of the friction cone length, inside the material 2.

The influence of Poisson's ratio v on the ζ is also examined. For v is equal to 0·0, 0·1, 0·2, 0·3, 0·4, or 0·5, the ζ is equal to 0·56, 0·58, 0·59, 0·61 or 0·65, respectively. The ζ is smoothly increased by 15·6 per cent with the increase of Poisson's ratio from 0 to 0·5. This result may indicate that soil compressibility has a limited effect on the cone sleeve friction resistance and is consistent with the fact that the friction resistance is dominated by soil shear deformation.

APPLICATIONS

Further, two examples are given to illustrate the application of the layered elastic model to the interpretation of CPT tip and sleeve friction resistance in layered soils. The first application is to analyze an actually measured CPT tip and sleeve friction resistance using the layered elastic model. Figures 7 and 8 show the results of the application. The measured tip and friction resistance q_c and f_s were obtained with a piezocone at a station site along the Lantau railway associated with the construction of Hong Kong new airport. Drillholes revealed that the ground soils comprised 6–13 m thick fill, 1–3 m thick marine deposit and 2–3 m thick completely decomposed granite, and were underlain by moderate to slightly decomposed granite. The fill materials also have layered structures consisting of medium dense slightly clay fine to medium sand, firm slightly sandy silty clay, dense silty fine to coarse sand, or fine to coarse gravel.

To simulate the measured tip resistance in Figure 7, the ground soils are modeled using a 14-layered elastic half-space. Following parameters were used in the evaluation: (a) the layer thicknesses t_i/a are equal to 288, 15, 7, 128, 20, 27, 5, 22, 15, 10, 30, 15, 20, 20, or ∞; (b) the layer shear modulus ratios μ_i/μ_l are equal to 1, 2·5, 16, 1·2, 20, 15, 10, 7, 15, 10, 15, 8, 2, 6, or 1·5; and (c) the Poisson's ratios v_i of the layers are equal to 0·3, 0·5, 0·5, 0·3, 0·5, 0·3, 0·3, 0·3, 0·3, 0·5, 0·5, 0·5, 0·5,

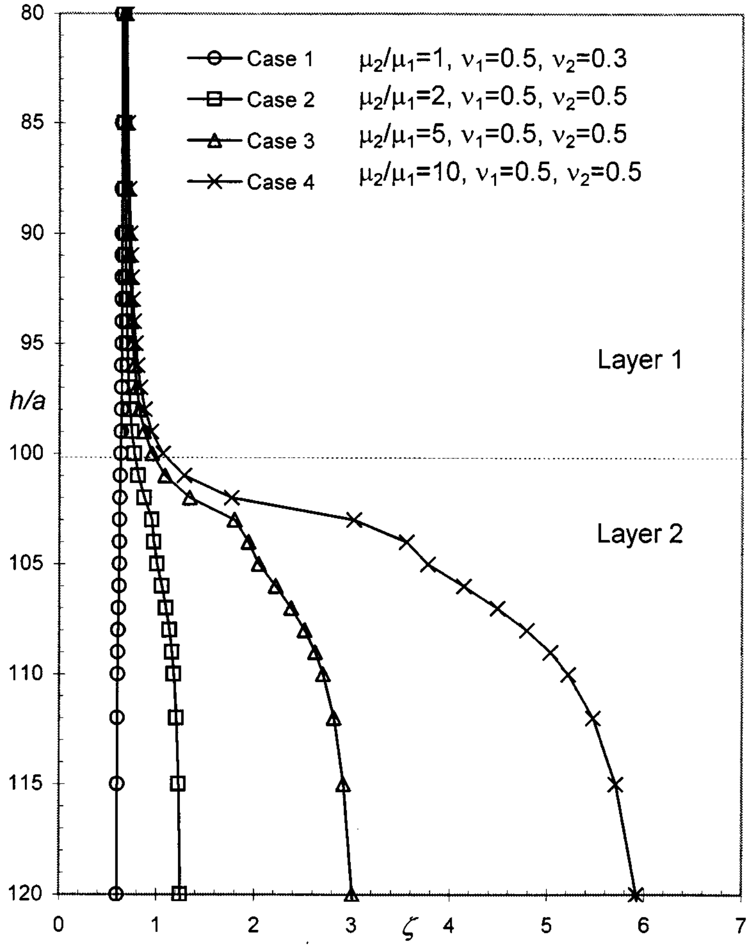

Figure 6. Variations of the non-dimensional sleeve friction ζ with the cone tip depth h/a in bi-material soils

0·5, or 0·3, for $i = 1, 2, \ldots,$ or 15, respectively. The measured friction resistance q_c in Figure 7 was non-dimensioned by a factor 2·12 MPa. From Figure 7, it can be observed that the *in situ* measured data are compared well with the predicted η values, despite the noisiness being in measured traces.

To simulate the measured sleeve friction resistance in Figure 8, the ground soils are also modelled using the above 14 layered elastic half-space. In Figure 8, the measured friction resistance f_s was non-dimensioned by a factor 23 kPa. From Figure 8, it can be observed that the predicted ζ values are not too far away comparing with the *in situ* measured data. The prediction is significantly improved by modifying the layered model as a seven-layered elastic half-space with the parameters: (a) $t_i/a = 288, 22, 128, 27, 62, 40, 50,$ or ∞; (b) $\mu_i/\mu_l = 1, 30, 1{\cdot}2, 22, 4, 20, 5,$ or 1·5; and (c) $v_i =$ 0·3, 0·5, 0·3, 0·5, 0·3, 0·5, 0·5, or 0·3 for $i = 1, 2, \ldots,$ or 8, respectively.

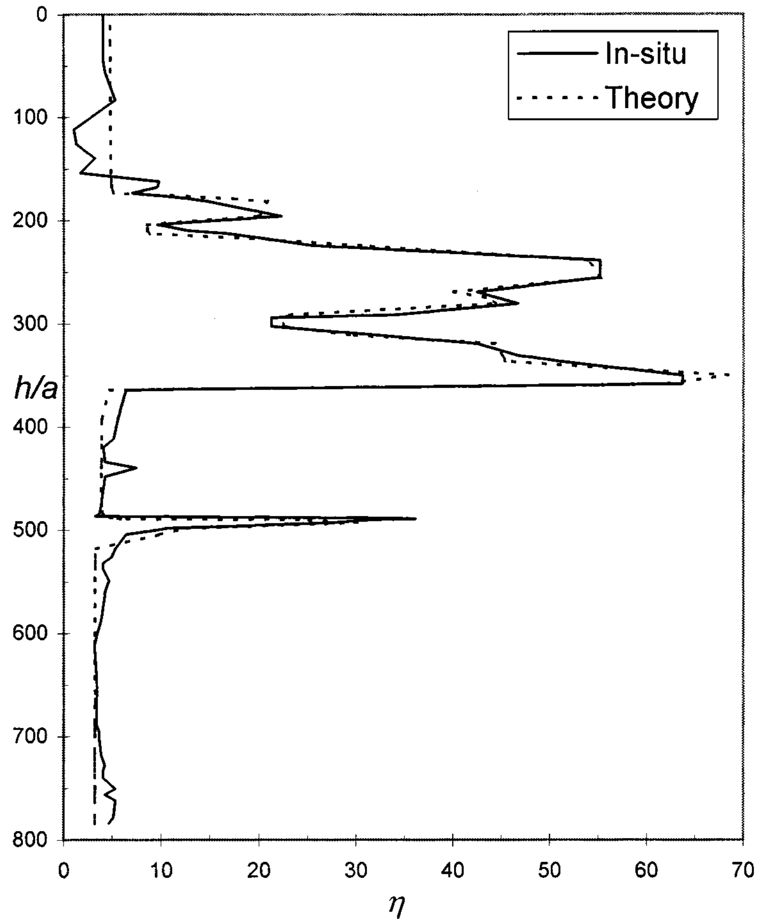

Figure 7. Simulation of an *in situ* cone tip resistance result using the layered elastic model

The second application is related to the layered elastic analysis of an incompressible clay layer over a compressible sand layer. Using a Eulerean large-strain finite element formulation, van den Berg *et al.*[18] presented a simulation in which a cone penetrated from an incompressible clay layer into a compressible sand layer. For the clay layer, the shear modulus μ, Poisson's ratio v, the cohesion c, the friction angle at constant volume ϕ_{cv}, the hardening/softening parameter κ and the dilatancy angle ψ were assumed equal to $671{\cdot}2\ \mathrm{kN/m^2}$, 0·49, $10\ \mathrm{kN/m^2}$, 0° and 0 and 0°, respectively. For the sand layer, μ, v, c, ϕ_{cv}, κ and ψ were assumed equal to $1923{\cdot}1\ \mathrm{kN/m^2}$,0·3, 2 kN/m2, 30°, 0·072, and 10°, respectively.

Figure 9 presents a comparison of the results given by van den Berg *et al.*[18] and obtained using the model presented above. The load–displacement curve for the clay layer on the sand layer in Figure 11 of Reference 18 was non-dimensioned using a factor 4/(0·15 MPa) and plotted in Figure 9, where 0·15 MPa is an approximated constant resistance in the clay layer. In the present study, an elastic layer of thickness ratio $t_1/a = 3{\cdot}5$ ($a = 17{\cdot}85$ mm) is assumed to represent the clay

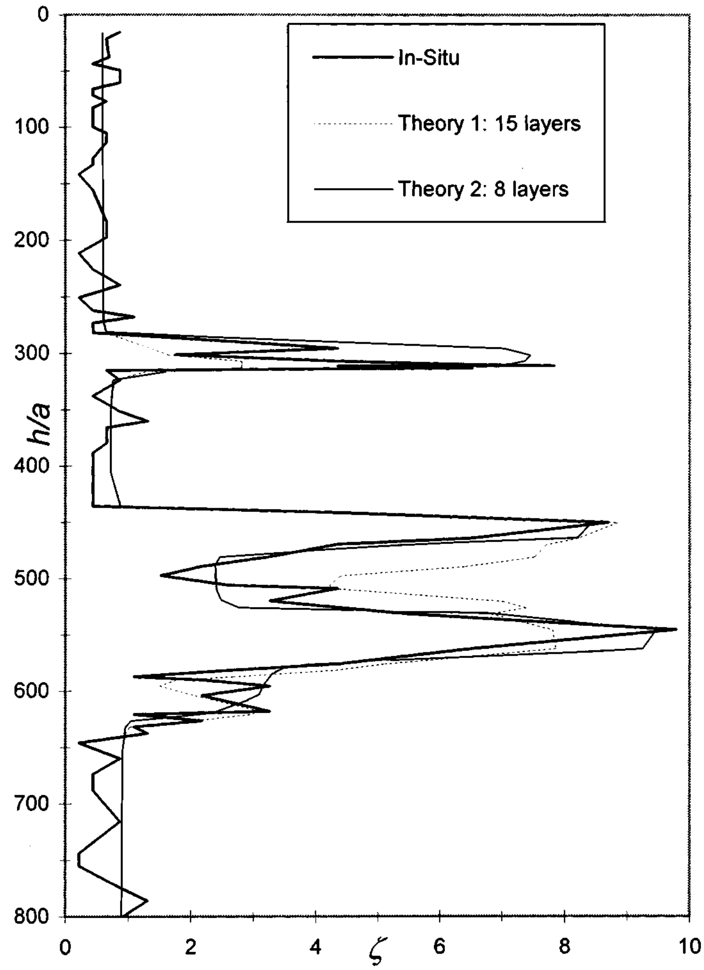

Figure 8. Simulation of an *in situ* cone friction resistance result using the layered elastic model

layer and an elastic half-space is used to represent the sand layer. Two sets of the elastic constant values are adopted in the present analysis. The first set is exactly the same as that used by van den Berg *et al.* (1996) namely: $\mu_2/\mu_1 = 2{\cdot}8654\ (= 1923{\cdot}1/671{\cdot}2)$, $v_1 = 0{\cdot}49$, and $v_2 = 0{\cdot}3$. For the second set, the shear modulus ratio μ_2/μ_1 is modified as 12·06.

From Figure 9, it can be observed that the η based on the present solution with the first set of shear modulus ratio is far lower than that given by van den Berg *et al.*,[18] while the η obtained using the present solution with the second set of shear modulus ratio has comparable values. Such results indicate that the layered elastic solution with the modified shear modulus ratio can be used to analyse the effect of a soft clay layer over a stiff sand layer on the cone tip penetration resistance. The modified shear modulus ratio represents a relatively overall strength of the clay and sand layers.

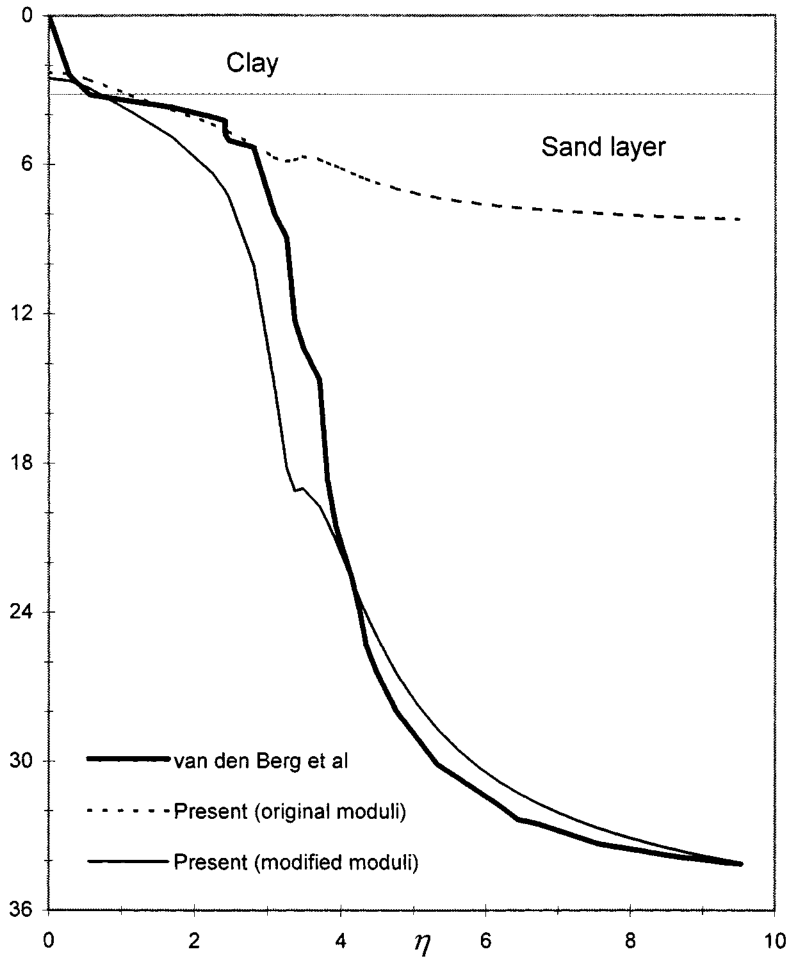

Figure 9. Compression of the present layered elastic results with large-strain finite element results for cone tip resistance in a clay layer over a sand layer

CONCLUSIONS

In the present study, a layered elastic model and associated solutions have been presented for the analysis of soil layering effects on the cone tip and sleeve friction resistance. The associated elastic solutions have been obtained by numerically integrating the fundamental singular solution for layered elastic solids due to a ring body force. The soil layering effects on the CPT results have been examined in detail by using the layered elastic model. These examinations include parametric studies, influence of soil compressibility, verification and comparison of the results given by others, simulation of experimental data and field trial results. Results of the examinations confirmed that the elastic approach proposed by Vreugdenhil *et al.*[16] can be used to the interpretation of soil layering effect on the CPT results. Furthermore, the shear modulus ratio of

elastic layers plays an essential role in the analysis of q_c and f_s while the soil compressibility has some effect on the tip resistance and a limited effect on the sleeve friction resistance. The estimated shear modulus ratio can be used as an index representing a relatively overall strength that soil layers exhibit during cone penetration.

ACKNOWLEDGEMENTS

Financial support from the Hong Kong Polytechnic University is acknowledged. The authors would also like to thank the referees for their constructive comments which enhanced the presentation of this paper.

REFERENCES

1. R. Butterfield and P. K. Banerjee, 'The elastic analysis of compressible piles and pile groups', *Géotechnique*, **21**(1), 43–69 (1971).
2. H. G. Poulos and E. H. Davis, *Pile Foundation Analysis and Design*, Wiley, New York, NY, 1980.
3. A. P. S. Selvadurai and R. K. N. D. Rajapakse, 'On the load-transfer from a rigid cylindrical inclusion into an elastic half-space', *Int. J. Solids Struct*., **21,** 1213–1229 (1985).
4. A. P. S. Selvadurai and M. C. Au, 'Generalized displacements of a rigid elliptical anchor embedded at a bi-material geological interface', *Int. J. Numer. Analyt. Meth. Geomech*., **10,** 633–652 (1986).
5. L. D. Ta and J. C. Small, 'Analysis of piled raft systems in layered soils', *Int. J. Numer. Anal. Meth. Geomech*., **20,** 57–72 (1996).
6. Z. Q. Yue and O. J. Svec, 'Effect of tire-pavement contact pressure distribution on the response of asphalt concrete pavements', *Canad. J. Civil Engng*. **25**(5), 849–860 (1995).
7. D. M. Burminstyer, 'Theory of stresses and displacements in layered systems and applications to the design of airport runways', *Proceedings of the Highway Research Board*, Vol. 23 1943.
8. D. M. Burminster, 'The general theory of stresses and displacements in layered systems I, I, III', *J. Appl. Phys*., **16,** 89–93, 126–127, 296–302 (1945).
9. Z. Q. Yue and R. Wang, 'Static solution for transversely isotropic elastic *N*-layered systems', *Acta Scientiarum Naturalium, Universitatis Pekinensis*, Beijing, **24,** 202–211 (1988) (in Chinese).
10. Z. Q. Yue, 'On generalized Kelvin solution in multilayered elastic medium', *J. Elasticity*, **40,** 1–43 (1995).
11. Z. Q. Yue, 'On elastostatics of multilayered solids subjected to general surface traction', *Quart. J. Mech. Appl. Math*. **49** (Part 3), 471–499 (1996).
12. Z. Q. Yue, 'Elastic field for an eccentrically loaded rigid plate on multilayered solids', *Int. J. Solids Struct*., **33**(27), 4019–4049 (1996).
13. G. M. Norris and R. D. Holtz (eds), *Cone Penetration Testing and Experience*, Proceedings of session sponsored by the Geotechnical Engineering Division at the ASCE National Convention, St. Louis, Missouri, 26–30 October, 1981.
14. A. C. Meigh, *Cone Penetration Testing: Methods and Interpretation* (CIRIA Ground Engineering Report: *In situ* Testing), Butterworths, London, 1987.
15. ASTM. 'Designation: D3441-94: Standard test method for deep, quasi-static, cone and friction-cone penetration tests', *ASTM Standard volume* 04·08: *Soil and Rock* (*I*): *D*420–*D*4914, American Society for Testing and Materials (ASTM), 1916, Race Street, Philadelphia, PA, 1995, pp. 338–344.
16. R. Vreugdenhil, R. Davis and J. Berrill, 'Interpretation of cone penetration results in multilayered soils', *Int. J. Numer. Analyt. Meth. Geomech*., **18,** 585–599 (1994).
17. P. Kiousis, P., G. Z. Voyiadjis and M. T. Tumay, 'A large strain theory and its application in the analysis of the cone penetration mechanism', *Int. J. Numer. Analyt. Meth. Geomech*., **12,** 45–60 (1988).
18. P. van de Berg, R. de Borst and H. Huétink, 'An Eulerean finite element model for penetration in layered soil', *Int. J. Numer. Anal. Meth. Geomech*., **20,** 865–886 (1996).
19. H. G. Poulos, 'Stresses and displacements in an elastic layer underlain by a rough rigid base', *Géotechnique*, **17,** 378–410 (1967).
20. Z. Q. Yue, 'Elastic fields in two joined transversely isotropic solids due to concentrated forces', *Int. J. Engng. Sci*. **33**(3), 351–369 (1995).
21. J. Canou, 'Piézocône et liquéfaction des sables, Rapport de synthèses des travaux réalisés au CERMES (1986–1988)', *Research Report, CERMES/ENPC*, Paris, 1989, 176 pp.
22. P. Foray and J. L. Pautre, 'Piézocône et liquèfaction des sables: synthèse des essais sur sites en Nouvelle-Zélande et des essais en Chambre de Calibration à I'IMG', *Research Report, IMG*, Grenoble, 1988, 70 pp.

